Ted Belytschko
Sang-Ho Lee
Departments of Civil Engineering and Mechanical Engineering
Northwestern University
Evanston, IL 60208

I-Sheng Yeh
Jerry I. Lin
Chen-Shyh Tsay
James M. Kennedy
KBS2 Inc.
Burr Ridge, IL 60521

Adaptivity in Crashworthiness Calculations

h-Adaptive finite element methods for nonlinear transient analysis by explicit time integration are described. Examples are given of adaptive calculations for simple components and prototype calculations for a full car model. h-Adaptivity offers substantial reductions in data preparation costs and improvements in accuracy. © *1993 John Wiley & Sons, Inc.*

INTRODUCTION

The major cost in crashworthiness analysis arises from model preparation. In many cases, two to three man-months or more are required to prepare the finite element model for a crash analysis. Some of this burden arises because of the inability to use existing linear models as a basis for the crash model, for usually considerable refinement is needed where severe deformations are expected, whereas coarse meshes are used for the rest of the model to save computer time. Furthermore, different models have to be developed for each of the crash scenarios that must be considered, which include frontal crash, rear impact, side impact, and others.

A substantial part of this burden can be alleviated by using adaptive procedures wherein the computer program automatically refines the mesh where it is needed for accuracy. Adaptive procedures for linear stress analysis and computational fluid dynamics are already available commercially, and have found enthusiastic acceptance. Although more computationally demanding than programs without adaptivity, they can save substantial amounts of engineering time.

This article describes some of the methods and experiences with two adaptive finite element programs for nonlinear transient analysis: WHAMS, a research program developed at Northwestern University and SUPERWHAMS, a commercial program developed by KBS2. The latter is an outgrowth of WHAMS. *h*-Adaptivity and its implementation is described. We cursorily address the issues of subcycling and contract-impact, which are essential for an effective implementation of *h*-adaptivity. The last sections give some numerical studies and concluding remarks.

ADAPTIVITY

The *h*-adaptive methodology for explicit nonlinear structural dynamics used here was described in Belytschko, Wong, Plaskacz (1989). In the *h*-adaptive process, elements are subdivided into smaller elements where more accuracy is needed; this process is called fission. The elements involved in the fission process are subdi-

Shock and Vibration, Vol. 1, No. 2, pp. 97–106 (1993)

CCC 1070-9622/93/02097-10

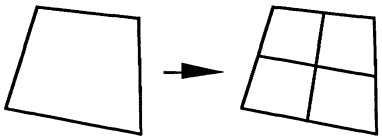

FIGURE 1 Fissioning of a quadrilateral element.

vided into elements with sides $h/2$, where h is the length of the side of the original elements. This is illustrated in Fig. 1 for a quadrilateral element. In fission, each quadrilateral is subdivided into four quadrilaterals (as indicated in Fig. 1) by using the midpoints of the sides and the centroid of the element to generate four new quadrilaterals. The fission process for a triangular element is shown in Fig. 2 where the element is subdivided into four triangles by using the midpoints of the three sides.

The adaptive process can consist of several levels of fission. Figure 1 shows one subdivision, which is called one level of adaptivity. In subsequent steps, the fissioned elements can again be fissioned in a second level of adaptivity, and these elements can again, in turn, be fissioned in a third level of adaptivity (Fig. 3). The number of levels of adaptivity is unrestricted, although it has been limited to three in most computations so far. The adaptivity in a mesh is restricted by three rules:

1. The number of levels is unrestricted in the program, but a maximum level of adaptivity is set in each calculation, which has been limited to three in our calculations.
2. The levels of adaptivity implemented in a mesh must be such that the levels of adaptivity implemented in adjacent elements differ by, at most, one level.
3. The total number of elements cannot exceed the limit specified by the user. Once the specified maximum number of elements is reached, no further fission is permitted.

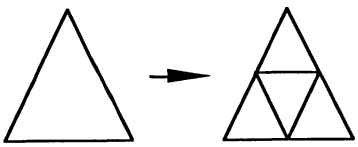

FIGURE 2 Fissioning of a triangular element.

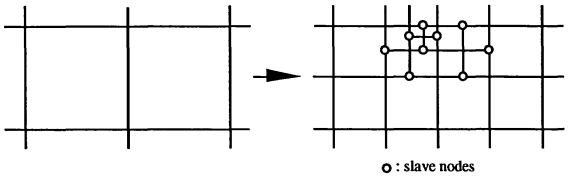

FIGURE 3 Quadrilateral element fissioned to third level; all nodes not labeled are master nodes.

The second rule is used to enforce a one-irregular rule given by Devloo, Oden, and Strouboulis (1987), which restricts the number of elements along the side of any element in the mesh to two. The enforcement of this rule is necessary to accommodate limitations in the data structure.

In WHAMS, elements were also fused or combined when it was felt that they were no longer needed. It was found that the implementation of fusion procedures for general meshes, such as occur in typical applications of commercial programs, is too complex, so only fission is included in SUPERWHAMS.

The original mesh provided by the user is known as the parent mesh, the elements of this mesh are called the parent elements, and the nodes are called parent nodes. Any elements that are generated by the adaptive process are called descendant elements, and any nodes that are generated by the adaptive process are called descendant nodes. Elements generated by the first level of adaptivity are called first-generation elements, those generated by the second levels of adaptivity are called second-generation elements, etc.

The coordinates of the descendant nodes are generated by using the midpoint of a line between immediate parent nodes. In subsequent steps, nodes that are not corner nodes of all attached elements are treated as slave nodes. They are handled by the tieline algorithm, which enforces compatibility of this node and consistently transfers its nodal forces to the adjacent master nodes.

Several error criteria have been studied. The first error criterion is an energy-normalized interpolation error criterion. The underlying motivation is a standard result in interpolation theory in one-dimension that for linear interpolants

$$\|u - u^h\| \leq \|u - u_I\| \leq Ch^2\|u_{,xx}\| \qquad (1)$$

where $\|\cdot\|$ is the L_2 norm, C is a constant, h is the characteristic element length, u is the function to be interpolated, and u_I the interpolate. We use

the arguments of Diaz, Kikuchi, Papalambros, and Taylor (1983) that the right-hand side can be approximated sufficiently by an interpolant u^* generated by the nodal values of u to indicate the error. Thus, the norm in the error can be approximated over a subdomain by

$$\|\text{error}\| = Ch^2\|u^*{}_{,xx}\|. \tag{2}$$

It can be shown for a plate in bending approximated by bilinear functions that the right-hand side in the above can be approximated by the change in angle between two elements. In order to obtain a normalized value, the change in angle is multiplied by the moment and divided by a suitable normalizing energy. The error indicator is then given by

$$e_{\text{indic}}^{\Delta\theta} = \Delta\theta m_\theta / \bar{W} \tag{3}$$

where $\Delta\theta$ is the change in angle across a side, m_θ a corresponding moment, and $\bar{W}$ the normalizing energy.

The other error indicators we used are of the Zienkiewicz–Zhu type. Lee (1993) has implemented an error criterion based on Zienkiewicz and Zhu's superconvergent patch (1992a,b), while Yeh (1992) has used an error criterion based on a global L_2 projection.

A difficulty in both cases is that the components of the stresses and strains in contiguous elements do not refer to a common coordinate system. In corotational elements, the stress and stain components are referred to corotational coordinates that differ between adjacent elements; even in total Lagrangian formulations for shells, the local coordinates systems of adjacent shell elements differ.

Therefore, the error indicator was expressed in terms of the invariants of the strains

$$e_{\text{indic}} = \int_{\Omega_e^T + \Omega_e^B} \sum_{i=1}^{3} [I_i^*(x) - I_i^h(x)]^2 dA \tag{4}$$

where I_i^h are the strain invariants computed by the finite element procedure and I_i^* are the strain invariants computed by the projection. The error indicator is obtained by integrating with 2×2 quadrature over the top and bottom surfaces of the shell element, which are indicated by Ω_e^T and Ω_e^B, respectively. Integrating over the volume is substantially more expensive and does not improve results.

In Lee (1993), the projected invariants I_i^* were obtained by using a local patch of four elements using a least squares fit of a bilinear polynomial to the superconvergent points of the finite element solution. Thus

$$I_i^*(x) = \mathbf{P}(x)\mathbf{a}_i \tag{5}$$

where

$$\mathbf{P}(x) = [1, x, y, xy] \tag{6}$$

and $\mathbf{a}_i$ are four parameters obtained by minimizing J given by

$$J = \sum_{Q=1}^{4} \sum_{i=1}^{3} [I_i^*(\mathbf{x}_Q) - I_i^h(\mathbf{x}_Q)]^2 \tag{7}$$

where $\mathbf{x}_Q$ are the superconvergent points of the elements, which correspond to the quadrature points in one-quadrature point elements. The coordinates x and y are measured on a projected plane by a stretching-mosaic technique. In Belytschko and Yeh (1992), a global L_2 projection was used to obtain I_i^*. Global projections are not as accurate as local projections (Zienkiewicz and Zhu, 1992a,b), so their efficacy as error indicators diminishes.

A fourth error criterion is obtained by first fitting the displacements at the nodes by a polynomial. The strains can then be computed by the strain-displacement equations. An error criterion is given by

$$e_{\text{indic}} = \int_{\Omega_e^T + \Omega_e^B} \|\varepsilon^*(x) - \varepsilon^h(x)\| dA \tag{8}$$

where ε^h is the finite element strains.

Note that in Eqs. (4) and (8), a total measure of strain must be used. In these programs, like in DYNA-3D, deformation is measured by the rate-of-deformation tensor, so to obtain a path independent measure of strain, the Green strain tensor is used for the error calculations.

The process of determining whether to fission any elements is called an assessment or judgment. Because the assessment process and associated remeshing is time consuming, it should not be done frequently in a run (maybe 5–20 times). In the assessment process, the error indicators are computed for all elements and sorted. Those elements that have error indicators that exceed the user–input tolerance are fissioned, provided that the total number of elements does not exceed the limit set on the number of elements.

Table I. Graphical Explanation of Go-Back Adaptive Algorithm

```
        Tw      TA
mesh 0 -------
                Tw      TA
mesh 1 ------- -------
                        Tw      TA
mesh 2          ------- -------
TIME ------------------------------------->
(×FA) 0         1       2       3
```

F_A: Frequency of assessments
T_w: Time along the solid analysis path at which the temporary analysis results are saved, then used for the repeat
T_A: Time along the dashed analysis path at which the adaptive assessment is done and, once a new mesh has been obtained, go back to T_w
—: Analysis path along which the results are the accepted results
—: Analysis path along which the results are only used for the adaptive assessment

It has been found through many numerical studies that to continue forward in time with the refined (or fissioned) mesh is often insufficient to achieve the benefits of adaptivity. The reason for this is that violation of the error criterion indicates that significant errors have occurred since the last assessment. Therefore, a procedure indicated in Table 1 is adopted. As can be seen from Table 1, whenever a judgment or assessment is made, the resulting finite element mesh is used to repeat the solution from the previous judgment. The output obtained by the coarser mesh is not retained; solutions that are not retained are indicated by dashed lines in Table 1. The final output stream of time histories then consists of the mesh-time path indicated by solid lines in Table 1.

SUBCYCLING AND CONTACT-IMPACT

When h-adaptivity is implemented with explicit time integration, mixed time integration (often called subcycling) is crucial for efficiency because the addition of smaller elements by fission reduces the stable time step (by a factor of 8 for three levels of fission). In WHAMS and SUPERWHAMS, mixed time integration as described in Belytschko and Liu (1982) is available. With this method, the time steps vary throughout the mesh so that each element is integrated with an optimal time step.

Contact-impact in an adaptive method is facilitated by a simple algorithm called the pinball method (Belytschko and Neal, 1991). The pinball algorithm embeds a sphere in each element, regardless of whether it is a shell or solid element, and then makes an interpenetration check by determining whether the pinballs have overlapped. This is a very simple check, because it only involves a comparison of the current distance between the pinballs with the sum of the radii. In the penalty form of the algorithm, whenever overlap of pinballs is detected, equal and opposite forces proportional to the magnitude of the interpenetration are then applied to the centers of the pinballs. These forces are then transferred to the nodes of the elements in which the pinball is embedded. Because the algorithm is very simple and identical regardless of what type of contact is involved, it is very amenable to vectorization and leads to very fast contact-impact algorithms. For example, the collapsing box beam problem that Zhong (1988) reported to take 64 min of CPU was solved in 16 min by the pinball algorithm. Only 15% of the total CPU time was expended by the pinball algorithm on a CRAY-YMP. In comparison to the Belytschko–Lin (1987) algorithm, the pinball algorithm was 5 times as fast on a vector compiler, 1.25 times as fast on a scalar compiler.

This algorithm was first developed to facilitate the vectorization of contact-impact algorithms for high velocity impact and penetration of solids in which erosion of elements occurs. It became apparent in subsequent work that the pinball method has a striking superiority: it is not necessary to distinguish different types of contact, because edge to surface and surface to solid contact can all be treated by the same algorithm (Belytschko and Yeh, 1993). Therefore the user can be spared from guessing the types of contact that may occur. Moreover, the applicability of a single algorithm to all contacts that occur in a model obviously facilitates vectorization.

NUMERICAL EXAMPLES

Several examples are given to demonstrate the performance of h-adaptivity. The formulations of the elements used here are given in Belytschko, Lin, and Tsay (1984) and Belytschko, Wong, and Chiang (1992). The materials used in the sample

Table II. Material Properties for Examples

Material Properties	Box Beam	S-Beam	Cylindrical Panel
Elastic modulus (E)	2.06×10^{11} N/m^2	3.00×10^7 psi	1.05×10^7 psi
Plastic modulus (E_p)	6.30×10^8 N/m^2	0.00 psi	0.00 psi
Yield stress (σ_y)	2.00×10^8 N/m^2	3.60×10^4 psi	4.40×10^4 psi
Density (ρ)	7.84×10^3 kg/m^2	7.40×10^{-4} lb.-s^2/in.^{4}	2.50×10^{-4} lb.-s^2/in.^{4}
Poisson's ratio (ν)	0.30	0.30	0.33

analyses are elastic-plastic with isotropic strain hardening; their properties are listed in Table 2.

The first example problem is a thin-walled box beam that impacts a fixed rigid wall. Figure 4 gives the geometry for this problem. It was previously analyzed by Benson and Hallquist (1987), Zhong (1988), and Belytschko and Neal (1991). Because of symmetry, only one quarter of this beam is modeled. Note that contact can occur between any two elements. Although roundoff error will sometimes trigger buckling even in symmetric structures such as this box beam, we found that the buckling modes can vary widely unless an imperfection is used to seed the buckling mode. An imperfection with different signs but the same magnitude on the sides and bottom as shown in Fig. 5 was used.

Figure 6 shows the rigid wall forces. Results from the fine nonadaptive meshes of 756 elements are used as our benchmark to show the improvement by the adaptive method. The improvement of accuracy and reduction of CPU time by the user of the adaptive method are also shown in Fig. 6, from which we can see a 40% reduction of CPU time, yet the adaptive result still coincides with the fine mesh result. Figure 7 shows the evolution of the adaptive mesh with time.

Figure 8 shows an original coarse mesh and

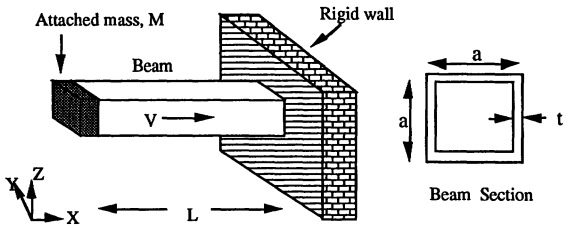

Geometry: L = 0.15 m, a = 0.03 m, t = 0.0015 m
Initial condition: V = 15.64 m/sec

FIGURE 4 Box beam problem.

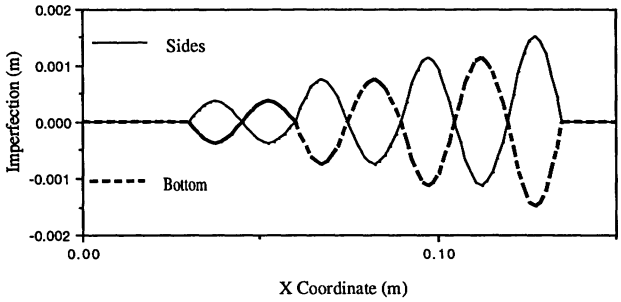

FIGURE 5 Imperfection distribution of the box beam.

adaptive results for an S-beam that strikes a rigid wall. Two levels of adaptivity were used. Note that refinement takes place at the corners where local buckling occurs. This local refinement substantially improves the accuracy of the solution.

The next example is a cylindrical panel that is loaded impulsively over a portion of the top surface; details of this problem are given in Kennedy, Belytschko, and Lin (1986). Experimental results have been reported by Balmer and Witmer (1964). Figure 9 shows the undeformed and deformed configurations at selected times and the deployment of elements by h-adaptivity; two

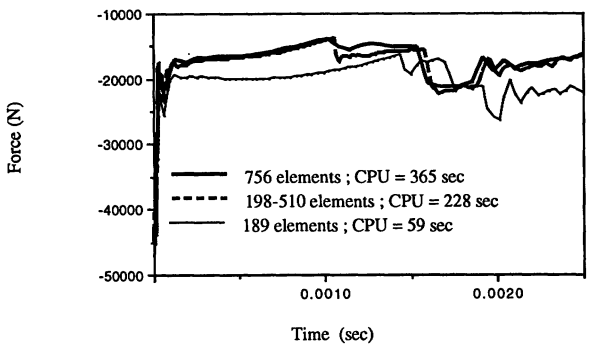

FIGURE 6 Time history of total force at the rigid wall for adaptive solutions.

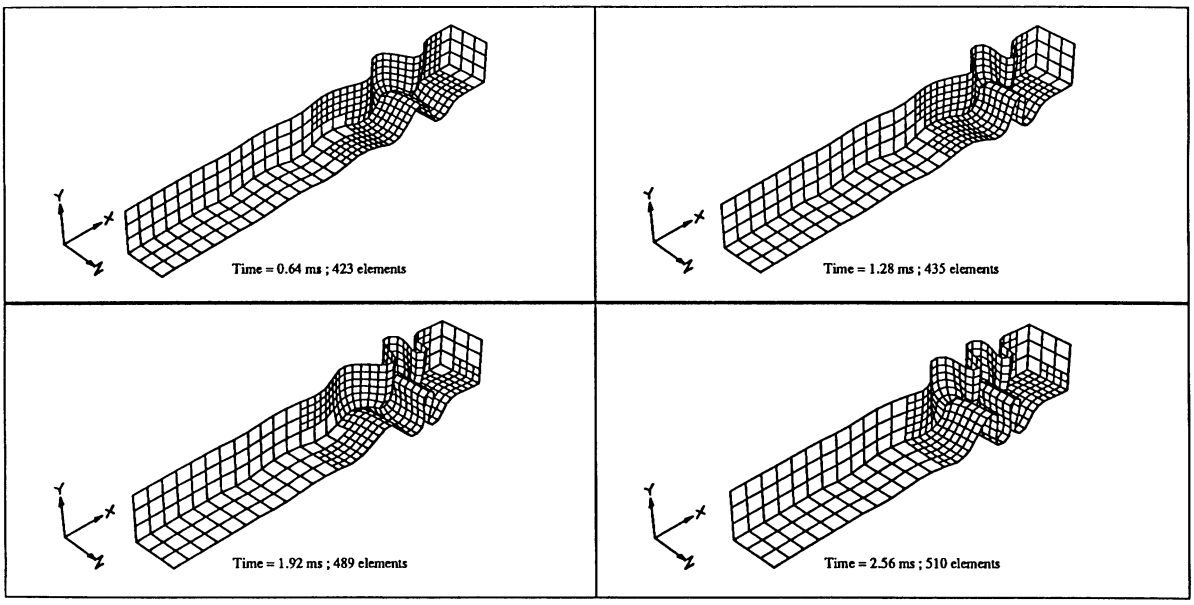

FIGURE 7 Deformed shapes of the box beam.

levels of subdivision were used along with the error criterion of Lee (1993).

Table 3 gives the maximum displacements for several nonadaptive meshes and adaptive meshes. The experimental results are also given. Note the improvement in accuracy for h-adaptivity. Experimental results are not an ideal benchmark for assessing adaptivity because discrepancies between experimental and numerical results may arise from inadequacies in the material law, such as neglecting strain-rate effects, and uncertainties in material properties, loading, and boundary conditions. Therefore, results obtained on a massively parallel computer, the CM-2, are included as the benchmark. Note that the adaptive results converge much faster to the CM-2 benchmark than fixed meshes. It is also interesting that meshes with the resolution often used in crashworthiness (8 × 16) exhibit large error. These errors can be explained by the inability of the coarse mesh to resolve the elastic-plastic hinge lines.

Table III. Results for Cylindrical Panel (With and Without Adaptivity)

Mesh	Description	Max. Central Deflection (in.)
8 × 16	Uniform	1.106
15 × 20	Uniform	1.140
15 × 20	Level 1 adaptivity	1.211
15 × 20	Level 2 adaptivity	1.238
16 × 32	Uniform	1.194
30 × 40	Uniform	1.220
126 × 256	Uniform	1.264
Experiment		1.280

We next discuss several crashworthiness calculations. Table 4 shows the timings with and without subcycling. As can be seen, the running time decreases by a factor of more than 2 with subcycling. Figure 10 shows the front end of a full model of a Ford van used for a frontal crash simulation with SUPERWHAMS. A modified pinball method was used for contact-impact; note that it effectively prevents interpenetration. A hypothetical rear end simulation (the rear end model does not contain the engineering detail required for a realistic analysis) was used for a two car collision. The model required about 90,000 elements. Running time increased by about a factor of 2 for the adaptive calculation as compared to the coarse mesh solution. However, this mesh could subsequently be used for similar rear end simulations at far less cost.

Figure 11 shows a portion of a side rail taken from a full car model solved with an adaptive mesh with one level of adaptivity; the deformed original coarse mesh is also shown. Note the significantly larger deformations of the h-adaptive mesh, which is also reflected in increased overall crush and lower acceleration levels.

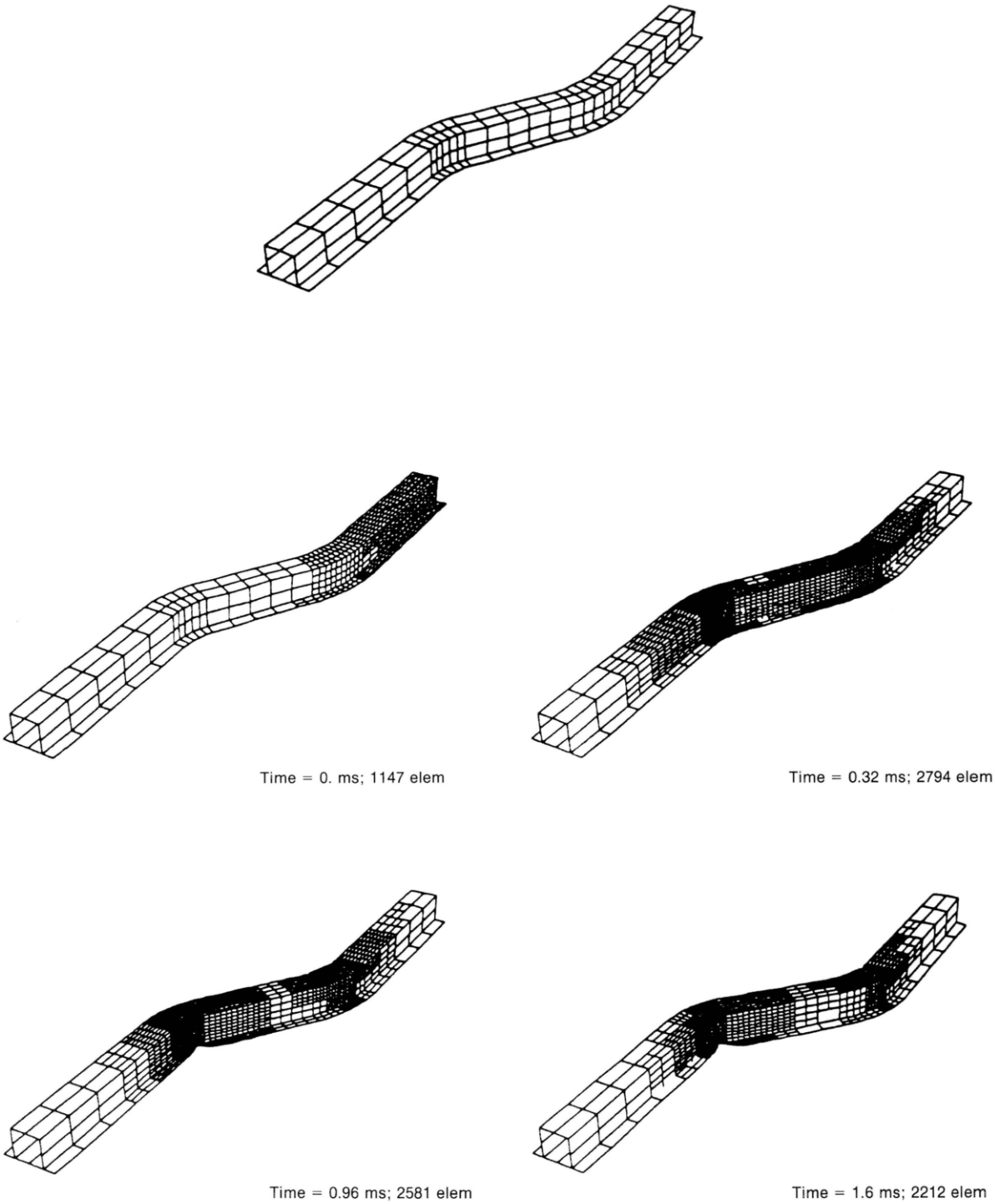

FIGURE 8 An original coarse mesh and adaptive results for the S-beam.

Table 5 gives the breakdown of the CPU time required by various parts of the SUPERWHAMS program in a crashworthiness analysis. With the pinball algorithm, only 15% of running time is attributable to the contact-impact algorithm. In some explicit codes, more than 60% is often required for the contact-impact algorithm in crash analysis. Thus the pinball algorithm saves substantial time in the calculation of contact-impact.

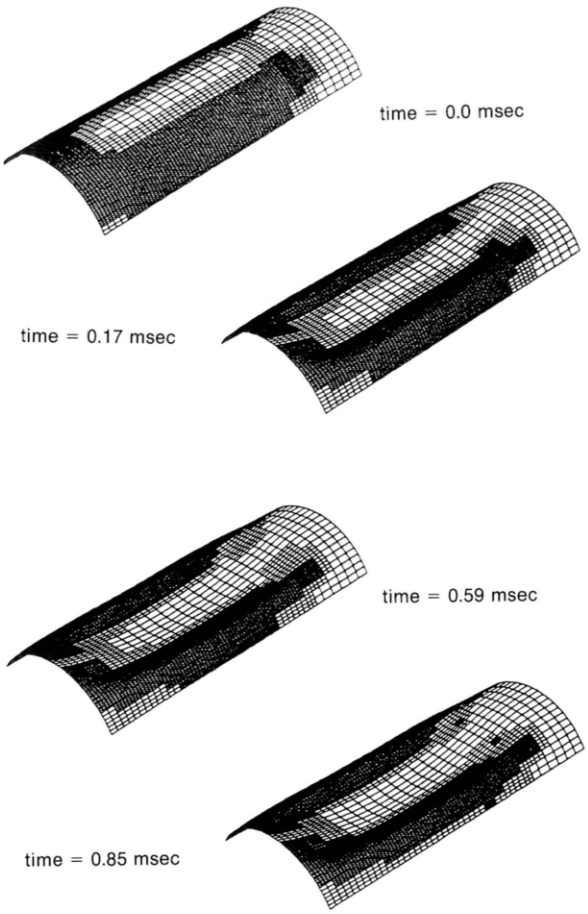

FIGURE 9 Deformed shapes of 120 degree cylindrical panel.

Table V. Breakdown of Time Required in Full Car Model Simulation for Various Functions on a Vector Processor

Function	Percentage of CPU Time	Degree of Vectorization
Element calculation	33.7	92.3
Pinball contact-impact	16.1	83.8
Material law	9.1	91.6
Time integration	5.3	80.6

CONCLUSIONS

Adaptive finite element techniques that are applicable to crashworthiness analysis have been described. Such analyses have a substantial potential for reducing model data preparation time and improving the quality of results.

The state of crash simulation today still requires considerable model tuning in order to match test results. Some of this tuning is probably due to insufficient resolution in the models. As illustrated by the simple cylindrical panel problem, very fine meshes are needed where plastic hinge lines occur to achieve good accuracy. The resolution of current finite element models for crashworthiness does not approach this level, and it is not possible with uniform meshes because of excessive computational costs. Limitations on sizes of models do not arise only from excessive computer time; computer memory requirements are also an important barrier. Adaptive methods have the potential for overcoming this accuracy barrier; by concentrating refinement where it is needed, high resolution and accuracy can be achieved with reasonable computer resources.

Multi-time step integration, often called subcycling, is an essential element for efficient *h*-adaptivity in explicit programs. Without subcycling, the local refinement of the mesh will re-

Table IV. Timings on Car Model

Elements	17,297	24,134
Time steps	78,274	43,680
	CRAY-YMP	FUJITSU VP-100
Without subcycling	7.63 h	9.48 h
Element cycle time	20 μs	32 μs
With subcycling	4.39 h	4.57 h
Effective element cycle time	12 μs	14 μs
Speedup	1.7	2.1
		VP-2600
With subcycling		0.91 h
Effective element cycle time		3 μs

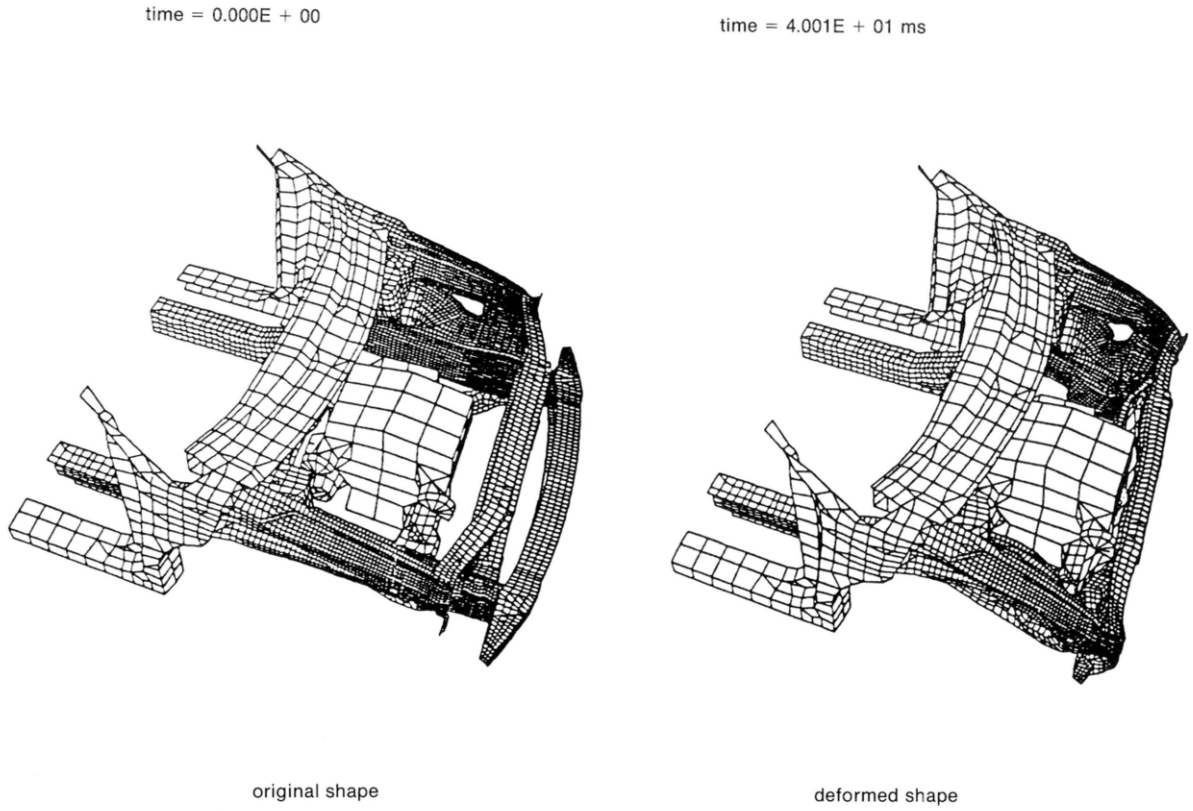

FIGURE 10 Original and deformed shapes of a vehicle front end with pinball contact-impact algorithm.

duce the time step over the entire mesh, which negates much of the advantage of adaptivity. Even without adaptivity, subcycling can provide savings of a factor of two in crash simulations.

We gratefully acknowledge the support of the U.S. Office of Naval Research and the National Center for Supercomputer Applications at the University of Illinois for computer time.

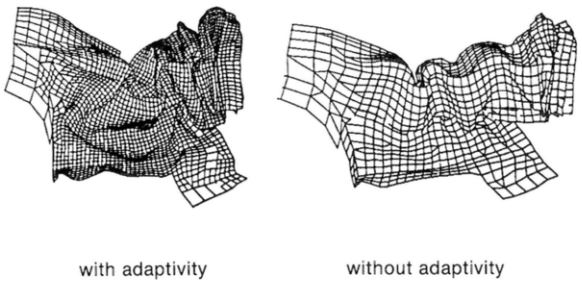

FIGURE 11 Component from a full car model showing deformation with and without adaptivity.

REFERENCES

Balmer, H. A., and Witmer, E. A., 1964, "Theoretical-Experimental Correlation of Large Dynamic and Permanent Deformation of Impulsively Loaded Simple Structures," Air Force Flight Dynamics Laboratory, Report FDP-TDR-64-108.

Belytschko, T., and Lin, J. I., 1987, "A Three Dimensional Impact-Penetration Algorithm with Erosion," *Computers and Structures,* Vol. 25, pp. 95–104.

Belytschko, T., Lin, J. I., and Tsay, C. S., 1984, "Explicit Algorithms for the Nonlinear Dynamics of Shells," *Computer Methods in Applied Mechanics and Engineering,* Vol. 42, pp. 225–251.

Belytschko, T., and Liu, W. K., 1982, "Time Integration with Explicit/Explicit Partitions in EPIC-2," Report to Ballistics Research Laboratory.

Belytschko, T., and Neal, M. O., 1991, "Contact-Impact by the Pinball Algorithm with Penalty and Lagrangian Methods," *International Journal for Numerical Methods of Engineering,* Vol. 31, pp. 547–572.

Belytschko, T., Wong, B. L., and Chiang, H. Y., 1992, "Advances in One-Point Quadrature Shell

Elements," *Computer Methods in Applied Mechanics and Engineering,* Vol. 96, pp. 93–107.

Belytschko, T., Wong, B. L., and Plaskacz, E. J., 1989, "Fission-Fusion Adaptivity in Finite Elements for Nonlinear Dynamics of Shells," *Computers and Structures,* Vol. 33, pp. 1307–1323.

Belytschko, T., and Yeh, I. S., 1992, "Adaptivity in Nonlinear Structural Dynamics with Contact-Impact," in A. K. Noor, AMD-Vol. 157, *Adaptive, Multilevel, and Hierarchical Computational Strategies,* American Society of Mechanical Engineers, New York.

Belytschko, T., and Yeh, I. S., 1993, "The Splitting Pinball Method for Contact-Impact Problems," *Computer Methods in Applied Mechanics and Engineering,* Vol. 105, pp. 375–393.

Benson, D. J., and Hallquist, J. O., 1987, "A Single Surface Contact Algorithm for the Postbuckling Analysis of Shell Structures," Report to the University of California at San Diego, CA.

Devloo, J., Oden, J. T., and Strouboulis, T., 1987, "Implementation of an Adaptive Refinement Technique for the SUPG Algorithm," *Computer Methods in Applied Mechanics and Engineering,* Vol. 61, pp. 339–358.

Diaz, A. R., Kikuchi, N., Papalambros, P., and Taylor, J. E., 1983, "Design of an Optimal Grid for Finite Element Methods," *Journal of Structural Mechanics,* Vol. 11, pp. 215–230.

Kennedy, J. M., Belytschko, T., and Lin, J. I., 1986, "Recent Developments in Explicit Finite Element Techniques and Their Application to Reactor Structures," *Nuclear Engineering and Design,* Vol. 97, pp. 1–24.

Lee, S.-H., 1993, "Nonlinear Transient Analysis Using *h*-Adaptivity and Pressure Stabilization," Ph.D. Thesis, Northwestern University, Evanston, IL.

Yeh, I. S., 1992, "Adaptivity and Splitting Pinball Method in Nonlinear Structural Dynamics with Contact-Impact," Ph.D. Thesis, Northwestern University, Evanston, IL.

Zhong, Z. H., 1988, "A Contact Searching Algorithm for General 3-D Contact-Impact Problems," Dissertation no. 178, Linkoping Institute of Technology.

Zienkiewicz, O. C., and Zhu, J. Z., 1992a, "The Superconvergent Patch Recovery and a posteriori Error Estimates. Part 1: The Recovery Technique," *International Journal for Numerical Methods of Engineering,* Vol. 33, pp. 1331–1364.

Zienkiewicz, O. C., and Zhu, J. Z., 1992b, "The Superconvergent Patch Recovery and a posteriori Error Estimates. Part 2: Error Estimates and Adaptivity," *International Journal for Numerical Methods of Engineering,* Vol. 33, pp. 1365–1382.